

Review

Design and Control of Cooperativity in Spin-Crossover in Metal–Organic Complexes: A Theoretical Overview

Hrishit Banerjee ¹, Sudip Chakraborty ² and Tanusri Saha-Dasgupta ^{1,*}

¹ Department of Condensed Matter Physics and Material Sciences, S N Bose National Centre for Basic Sciences, JD Block, Sector III, Salt Lake, Kolkata 700106, India; h.banerjee10@gmail.com

² Materials Theory Division, Department of Physics and Astronomy, Uppsala University, Box 516, 75120 Uppsala, Sweden; sudiphys@gmail.com

* Correspondence: t.sahadasgupta@gmail.com; Tel.: +91-33-2335-5707

Academic Editor: Kazuyuki Takahashi

Received: 20 June 2017; Accepted: 14 July 2017; Published: 20 July 2017

Abstract: Metal organic complexes consisting of transition metal centers linked by organic ligands, may show bistability which enables the system to be observed in two different electronic states depending on external condition. One of the spectacular examples of molecular bistability is the spin-crossover phenomena. Spin-Crossover (SCO) describes the phenomena in which the transition metal ion in the complex under the influence of external stimuli may show a crossover between a low-spin and high-spin state. For applications in memory devices, it is desirable to make the SCO phenomena cooperative, which may happen with associated hysteresis effect. In this respect, compounds with extended solid state structures containing metal ions connected by organic spacer linkers like linear polymers, coordination network solids are preferred candidates over isolated molecules or molecular assemblies. The microscopic understanding, design and control of mechanism driving cooperativity, however, are challenging. In this review we discuss the recent theoretical progress in this direction.

Keywords: Spin-Crossover (SCO); stimulus-induced spin transition; crystal engineering of SCO and related complexes

1. Introduction

The phenomena of Spin-Crossover (SCO) has caught the attention of scientific community for ages and has shown growing interest in recent time due to various different application possibilities in the information technology [1], as sensors [2], optical switches [3], etc. The essence of the SCO phenomena is described in the following. SCO may take place in transition metal complexes, specially those consisting of transition metal ions and flexible organic ligands, wherein the spin state of the metal ion changes between low spin (LS) and high spin (HS) configuration under the influence of external perturbation [4]. Though this process, in principle, can be observed in any octahedrally or tetrahedrally coordinated transition metal complexes with transition metal ions in d^4 – d^7 or d^3 – d^6 electronic configurations, the most commonly observed cases are that of octahedrally coordinated iron(II) complexes with Fe^{2+} ions in $3d^6$ electronic configuration [5–7]. The transition between the paramagnetic high spin ($S = 2$) and the diamagnetic low spin ($S = 0$) state of Fe^{2+} can be triggered by several different possibilities such as temperature, pressure, light [8]. The SCO phenomenon deserves attention due to accompanying changes in magnetic and optical properties. To be of use in device applications, it is important to induce cooperativity in the SCO phenomena implying spin transition rather than spin crossover, which may happen with associated hysteresis effect as shown in Figure 1.

The issue of cooperativity and associated hysteresis is important as it is expected to confer memory effect to the system.

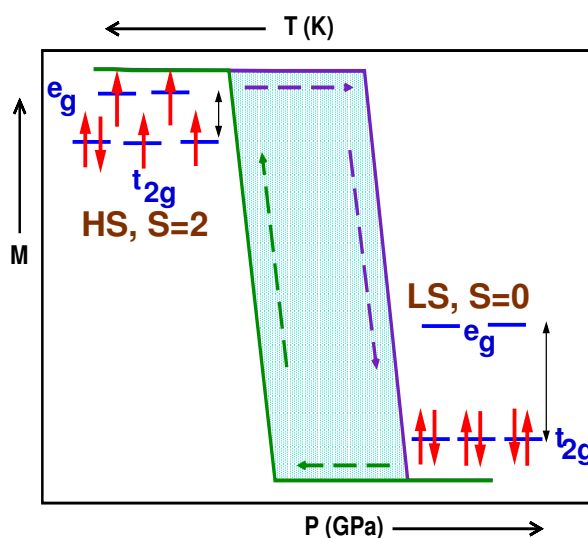


Figure 1. Schematic diagram demonstrating the cooperativity associated with spin crossover phenomena in Fe(II) complexes. The y axis shows the magnetic moment (M) and x axis represents temperature (T) or pressure (P) increasing in two different directions as shown in the figure. Upon increasing T or decreasing P , a transition happens from LS $S = 0$ state where all spins are paired up in the t_{2g} states octahedrally coordinated d^6 Fe, to HS $S = 2$ state where two of the electrons from t_{2g} states are promoted to e_g states. Due to the cooperativity between Fe(II) centres in the extended solid state geometry, hysteresis loop appears between the heating and cooling cycles, or between cycles of exertion and release of pressure.

In this context, in comparison to molecular assemblies or crystals with isolated molecular units connected by weak, van der Waals or hydrogen bonding, the coordination polymeric compounds with repeating coordination entities having extended solid structures are better choices. The presence of chemical bridges, linking the SCO sites to each other, as in coordination polymers are expected to propagate the interaction between SCO centers more efficiently than that in molecular crystals. Admitting the suitability of such compounds in exhibiting cooperativity there are several issues that need attention. The key questions are, (a) understanding the microscopic mechanism, i.e., what is the driving force for the cooperativity and the hysteresis; and (b) how the cooperativity can be tuned or modified to suit the specific need. These understandings are expected to provide an advancement of the field in terms of possible commercialization of this technologically important property which relies on critical parameters of cross-over being close to ambient condition, and a large enough hysteresis width.

The above two issues are also intimately connected to materials issue, namely what are the materials to look for cooperative SCO. As mentioned above, 1, 2 or 3-dimensional coordination polymers, which are materials with repeating array of coordination entities, are the suitable choices. The dimensionality of a coordination polymer is defined by the number of directions in space the array extends to. Most studied SCO materials showing cooperativity, so far are linear 1-dimensional coordination polymers which are compounds extending through repeating coordination entities in 1-dimension forming chain like structures, with weak links between individual chains [9], as shown in left panel of Figure 2. The other possibilities are coordination network solids [9], which are compounds extending through repeating coordination entities in 2 or even 3 dimensions. Strategic crystal engineering that makes use of multidentate ligands, connected by spacers, facilitates to increase the dimensionality from 1-d to 2-d or 3-d. Pressure-induced LS–HS transition in 2-d net was first reported for $[\text{Fe}(\text{btr})_2(\text{NCS})_2] \cdot \text{H}_2\text{O}$ [10]. The compound consisted of Fe(II) ions linked by btr in two directions producing infinite layers which were connected by means of van der Waals or weak H

bonds. $[\text{Fe}(\text{btr})_3][(\text{ClO}_4)_2]$ [11] represents the first 3-d SCO coordination polymer. For a concise review on 1-d, 2-d and 3-d Fe(II) polymers, please see Reference [11].

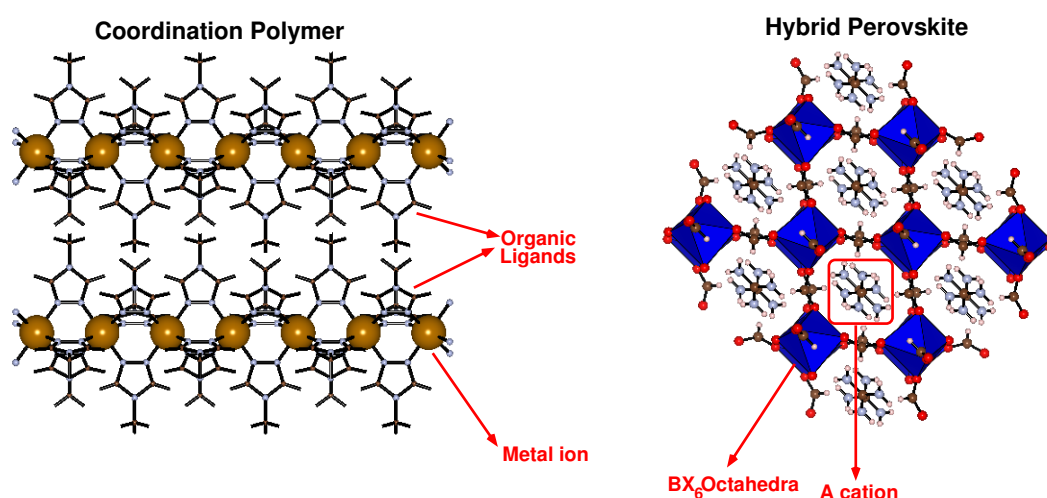


Figure 2. Schematic representation of linear, 1-d coordination polymer (**left** panel) and hybrid perovskite (**right** panel). In case of linear, 1-d coordination polymer, chains of metals are linked by organic ligands. In the ABX_3 structure of hybrid perovskite, BX_6 forms octahedra with A cation sitting in the voids. B cation is a metal ion and A cation is an organic cation. BX_6 octahedra are also linked by organic linkers.

For the sake of description of theoretical studies, we will restrict ourselves to only linear or 1-d coordination polymers, and not extending our discussion to 2-d or 3-d polymers of type $[\text{Fe}(\text{btr})_2(\text{NCS})_2] \cdot \text{H}_2\text{O}$ or $[\text{Fe}(\text{btr})_3][(\text{ClO}_4)_2]$. Rather we will focus in a new class of materials in context of SCO, namely hybrid perovskites. A subclass of coordination network solids are metal organic frameworks (MOFs) which are coordination networks with organic ligands containing potential voids [9], and thus can be labeled as porous coordination polymers. Most of the research on MOFs are related to porosity of the systems, which have been explored for applications in gas storage [12], chemical sensing [13], drug delivery [14], bio mimetic mineralization [14] and catalysis [15]. Recently, however, the attention is also given to dense MOFs with limited porosity which show potential for applications in other areas like optical devices, batteries and semiconductors [16]. Hybrid perovskites are a class of compounds with general formula ABX_3 having long range connectivity that form a subclass of dense MOFs. The extended, 3-dimensional connectivity with limited void space, together with possibility of synthesizing hybrid perovskites containing transition metal ions have made these compounds also probable candidates for exhibiting cooperative SCO. While linear coordination polymers have already been explored to a large extend in search of cooperative SCO, ABX_3 type hybrid perovskites which though in attention in recent time has not been explored for cooperative SCO. In the following we give brief description of each of these classes of compounds, namely linear chain compounds, and hybrid perovskites.

Among the linear coordination polymers, or 1-d chain compounds 4R-1,2,4-triazole based Fe(II) chain compounds have been in focus both in early studies and in recent developments. $[\text{Fe}(\text{4R-1,2,4-triazole})_3]\text{A}_2 \cdot \text{solv}$, where A is the counterion and *solv* denotes the solvent molecule are made up of linear chains in which the adjacent Fe(II) ions in the chain are linked by three triazole ligands. The coordination linkers, which are 1,2,4-triazole blocks form efficient chemical bonds to transmit cooperative effect, leading to hysteresis loop of width ranging $\approx 2\text{--}20$ K. [17] Sometimes these hysteresis loops are also found to be centered at room temperature. [18] Bimetallic 1-d chain compounds like $\text{Fe}(\text{aqin})_2(\mu_2\text{-M}(\text{CN})_4)$, M = Ni(II) or Pt(II), have been recently synthesized which were found to show abrupt HS–LS SCO. [19] Novel 1-d Fe(II) SCO coordination polymers with 3,3'-azopyridine as axial ligand has been synthesized which were found to show kinetic trapping

effects and spin transition above room temperature. [20] Combination of rigid links and a hydrogen bond network between 1-d Fe(II) chains has been recently shown as a promising tool to trigger SCO with hysteresis loops having widths as large as ≈ 43 K. [21]

Hybrid perovskites [22,23] having general formula of ABX_3 , on the other hand, are counterparts of inorganic perovskites. In case of hybrid perovskites, while the B cation is a metal ion as in inorganic perovskites, both the A cation as well as the ligand can be organic. Lead halides hybrid perovskite family [23,24] having $[AmH]MX_3$ composition, where AmH^+ is the protonated amine part; M is either Sn^{2+} or Pb^{2+} and X is the halogen part (Cl^- , Br^- , or I^-) have been shown to demonstrate high performance and efficiency in applications relating to design of mesostructural (and/or nanostructural) solar cells and other photovoltaic devices [25–27]. Easy processing techniques like spin-coating, dip-coating and vapor deposition techniques have been known to be of advantage in this case [28,29]. There are also transition metal formate based hybrid perovskites, which are of interest in the present context, having formula $[AmH]M(HCOO)_3$ ($M = Mn, Cu, Ni, Fe, Co$). [30] In the crystal structure of these compounds, as shown schematically in right panel of Figure 2, formate bridges act as linkers that connect the MO_6 octahedra, with the protonated amine cations situated at the hollow spaces formed by the linked octahedra. These hollow spaces act as pseudo-cubic ReO_3 type cavities. Organic ligands like formate being simple enough have been mostly studied with varied A cations. This class of materials has been shown to exhibit curious properties, of which multiferroicity seems to be an intriguing one [31–33]. Ferroelectricity and especially multiferroicity in these materials has been extensively studied by Stroppa and coworkers mostly from a DFT based first principles perspective and at times combined with experimental studies [34–40]. Structural details and effects due to structural phase transitions, strain tuning of various effects like polarisation, and magnetic structure has also been studied by the same groups [41–45]. As mentioned already, the presence of transition metal in these compounds together with its octahedral environment makes them suited also for exhibiting SCO behavior and possibly also cooperativity due to dense nature of framework, which would provide another dimension to functionality of these interesting class of compounds. This aspect of this interesting class of compounds has remained unexplored, apart from a very recent theoretical proposal [46].

The plan of the review is the following. We will start with a brief summary of the experimental investigations on cooperative SCO, as presented in Section 2. With this background, we will discuss in Section 3 different theoretical models that have been proposed to describe cooperative SCO. In Section 4, we will take up the material specific studies, where density functional theory (DFT) based electronic structure calculations have been employed to investigate cooperative SCO phenomena in well studied case of linear coordination polymer and proposed case of hybrid perovskite. We will conclude the review with a summary and outlook in Section 5, where the future prospective and challenges that needs to be overcome will be discussed.

2. Experimental Evidences of Cooperativity

During the past few decades, there has been a growing number of experimental studies focusing on spin crossover phenomena in general. Numerous studies have been carried out on various materials ranging from molecules to molecular assemblies to coordination polymers, linear coordination polymers being the most studied case in latter category. In case of linear coordination polymers, often a significant hysteresis effect is observed, primarily under the influence of temperature, though there exists studies showing the existence of hysteresis in SCO under pressure. There have been also studies involving light-induced spin-crossover transitions. In the following we provide a brief over-view. Given the vastness of the experimental study on SCO, the over-view presented in the following is far from being complete and should be considered as representative. In the first part of the brief over-view, we provide description of experimental studies of SCO phenomena in general, while in the later part we specifically focus on cooperative SCO.

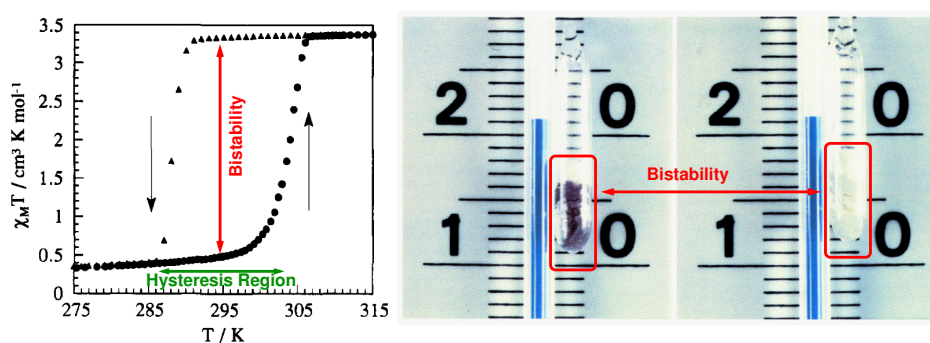


Figure 3. Experiment evidence of cooperativity in Fe-triazole, as reported by Kahn et al. [18] (Adapted with permission from Krober, J.; Codjovi, E.; Kahn, O.; Groliere, F.; Jay, C. A spin transition system with a thermal hysteresis at room temperature. *J. Am. Chem. Soc.* **1993**, *115*, 9810–9811). The **left** panel shows the variation of susceptibility with increasing and decreasing temperature. A large hysteresis loop and corresponding bistability is observed confirming the existence of cooperativity; The **right** panel demonstrates the bistability in the system, reflected in two different colors of the same material at the same temperature, being on cooling or heating path.

SCO phenomena was first reported in the pioneering work by Cambi et al. [47] as early as in 1931, in a series of Fe based metal–organic compounds viz. iron (III) tris-dithiocarbamate. In their study, the authors observed a transition from $S = 1/2$ to $S = 3/2$ spin state. Since then there have been subsequent experiments which demonstrate SCO in other materials, which are mostly Fe based compounds, but also in Co, Ni, Cr, and Mn based compounds [5–7,48]. König et al. [49] in 1961 first observed a $S = 0$ to $S = 2$ transition in a iron (II) thiocyanide material which later became a popular material of study in the area of spin crossover. Various experimental techniques have been employed to study the phenomena of spin crossover, the most popular one being magnetic susceptibility measurement. X-ray diffraction or Extended X-ray absorption Fine Structure (EXAFS) has been employed to measure the structural properties of SCO compounds. [50,51] Mössbauer Spectroscopy has been also employed to detect SCO in iron complexes. [49,52,53] Raman spectroscopy has been used to identify spin state of SCO complexes. [54] Fourier Transform Infrared Spectroscopy (FT-IR) has been employed to plot the area under the curves of the absorption peaks as a function of temperature which have been used to map out the SCO. [55] UV-vis spectroscopy has also been an important tool for detecting the changes of electronic states in SCO materials. [56] Electron Paramagnetic Resonance (EPR) [57], Muon Spin Relaxation (μ SR), Positron Annihilation Spectroscopy (PAS), Nuclear Resonant Scattering of synchrotron radiation (NRS) are among other techniques which have also been used for experimental study of SCO [58]. While for most experimental studies, the temperature or pressure has been used as external perturbation, there have been also several experimental studies on light induced spin crossover or as it is known Light induced spin state trapping (LIESST). This was first reported by Decurtins and coworkers. [59] In the work by Decurtins and coworkers, [59] the Fe(II) based compound was converted from stable LS state to metastable HS state at low temperature by irradiating the sample with green light. In a subsequent work, Hauser [60] reported the back conversion to LS state by irradiation of red light. It was found [59] that very low temperatures are required for trapping the system in the metastable HS state. The systems relaxes to the LS state above a critical temperature which was defined as $T_C(\text{LIESST})$ [61]. Estimation of the $T_C(\text{LIESST})$ value was found to give an idea of the capability of the material to store the light induced HS state. Superconducting quantum interference device (SQUID) magnetometer measurements were carried out in a study by Kahn et al. [61] to characterize LIESST and determine T_C values for the thermally induced SCO for a variety of Fe SCO materials. In this work correlation between the photomagnetic properties and the thermal properties of a variety of SCO materials was drawn. A plot of the $T_C(\text{LIESST})$ vs the spin crossover temperature for a collection of materials was found to show

a correlation between the two. It was concluded that the positioning of a given compound in plot is governed by the cooperativity of the compound.

Other than the case of molecular mononuclear moieties, a large number of studies involve one, two and three-dimensional coordination polymers with multiple SCO centers, exhibiting intriguing hysteresis effects. In a seminal experimental study by Kahn et al. [18] thermal hysteresis at room temperature was demonstrated in case of Fe-triazole compound, in particular $[\text{Fe}(\text{Htrz})_{3-3x}(\text{4-NH}_2\text{trz})_{3x}](\text{ClO}_4)_2 \cdot n\text{H}_2\text{O}$ with $x = 0.05$. As shown in Figure 3 the temperature dependence of measured susceptibility showed a spin state transition accompanied by a wide hysteresis loop close to room temperatures, as is desirable for commercial applications. As seen in the figure, the transition is also accompanied by a dramatic change of color. The two spin states correspond to two different electronic states exhibiting two different colors. Depending on whether the observation is being made in the heating or the cooling cycle, the sample at the same temperature falling within the hysteresis width exhibits two different colors, establishing the bistability of the two spin states. The molecular system described in this particular study was probably the first one of its kind exhibiting such a bistability at room temperature. This paved the way for future experimental and simulation based studies on cooperativity.

The experimental study by Linares et al. [62] which was also backed by simulation, reported the existence of hysteresis in SCO phenomena induced thermally as well as through pressure. Their experimental and simulation studies on $[\text{Fe}_x\text{Co}_{1-x}(\text{btr})_2(\text{NCS})_2] \cdot \text{H}_2\text{O}$ with $x = 0.847$ showed large hysteresis loops under heating and cooling cycle confirming cooperativity in these materials. Their study on $[\text{Fe}_x\text{Ni}_{1-x}(\text{btr})_2(\text{NCS})_2] \cdot \text{H}_2\text{O}$ with $x = 0.66$ showed large hysteresis in pressure induced SCO.

Baldé et al. [63] considered coordination polymers with the general formula $[\text{Fe}L_{eq}(L_{ax})] \cdot \text{solvent}$ where $L_{eq} = 3,3'$ -[1,2-phenylene bis(iminomethylidene)]bis(2,4-pentanedionato)(2-)-N,N',O²,O'² and 3 different components for L_{ax} such as 4,4'-bipyridine(bipy), 1,2-bis(4-pyridyl)ethane (bpea), and 1,3-bis(4-pyridyl)propane (bppa). Cooperative SCO was previously [64–66] reported for the bipy linker, which showed thermal hysteresis and bpea and bppa based compounds showed multi-step transitions. In the study by Baldé et al. [63] the authors also investigated the LIESST effects and estimated the $T_C(\text{LIESST})$ values by irradiating the samples in a SQUID. The thermal measurements showed hysteresis in bipy linker based compound with a 2 step transition in bpea based compound and a 2 step transition accompanied by hysteresis in bppa based compound. Evaluation of the $T_C(\text{LIESST})$ values associated with the LIESST effect demonstrated the stability of the photoinduced HS state. Experiments on $[\text{Fe}_x\text{Ni}_{1-x}(\text{btr})_2(\text{NCS})_2] \cdot \text{H}_2\text{O}$ with $x = 0.5$ by Linares et al. [62] under constant light exposure allowed the investigation of the competition between photoexcitation and subsequent relaxation of the metastable state, and a thermal hysteresis under constant light irradiation.

Numerous other studies on SCO compounds, apart from the ones described above, have been carried out which recorded hysteresis in thermal, pressure and light induced spin state transitions. For the sake of brevity, we will not get into the details of all the studies. The few studies described above provide conclusive evidences of experimental observation of cooperativity in SCO complexes.

3. Theoretical Models on Cooperativity

Several theoretical studies have been reported in literature with an aim to provide microscopic understanding of the origin of spin state transition and its cooperativity in metal organic complexes. While the spin crossover in molecular systems with a single SCO center happens due to competition between the crystal field splitting and Hund's rule coupling, in case of extended polymeric systems, interactions between different SCO centers may drive the cooperativity in SCO observed at molecular level. It is important to understand the microscopic origin of this interaction. This understanding is expected to enable designing of extended solid state structures with desired cooperative properties.

The most prevailing concept in this context, is that the interaction is given by phononic excitations due to coupling between local lattice distortions at each molecular unit, setting up a long range elastic wave. Two different model Hamiltonian approaches have been followed to deal with elastic

interactions between SCO centers to calculate thermodynamic quantities like HS fraction. In the first category of calculations, Ising type Hamiltonians, $H = \sum_{ij} J_{ij} \sigma_i \sigma_j$ are used with LS or HS state described by pseudo-spin operators $\sigma_i = -1(+1)$ for LS(HS) that interact via nearest neighbor elastic coupling. For example, the study by Boukheddaden et al. [67] considered one-dimensional spin-phonon model, which is expected to model the linear polymeric compounds. In particular the model consisted of assembly of two-level system with elastic interaction between them. The HS state, represented by pseudo-spin $\sigma = 1$ was assumed to be n_H fold degenerate, while the LS state represented by $\sigma = -1$ was assumed to be n_L fold degenerate. The elastic interaction linking the sites i and $i + 1$, was denoted by $e_{i,i+1}$. Volume of the molecule changes upon the spin state transition, and thus the elastic interactions between two successive sites was assumed to depend on their spin states. It was conjectured that $e_{i,i+1} = e_{++}$ for $\sigma_i = \sigma_{i+1} = 1$, $e_{i,i+1} = e_{+-}$ for $\sigma_i = -\sigma_{i+1}$, and $e_{i,i+1} = e_{--}$ for $\sigma_i = \sigma_{i+1} = -1$. The constructed model was solved in the framework of classical statistical mechanics using transfer matrix technique. The effective interaction turned out to be ferroelastic for $e_{+-} > \sqrt{e_{++} \times e_{--}}$ and antiferroelastic for $e_{+-} < \sqrt{e_{++} \times e_{--}}$, which in turn was found to be determining factor for the lattice of SCO centers to exhibit cooperativity or not. It was found that ferroelastic interaction favors cooperativity with sharp spin state transition while the antiferroelastic interaction makes the transition much smoother. This indicated that in presence of ferroelastic interaction, first-order phase transition along with hysteresis might take place in higher dimensions. The authors thus introduced inter chain interactions, justified by the fact that in SCO polymeric samples, interchain steric and electrostatic interactions arise due to presence of non-coordinated molecules or counter anions. The mean field treatment of interchain interactions indeed was found to reproduce the first-order nature of HS–LS transition together with hysteresis for ferroelastic intrachain interactions.

In the second category of calculations, free energy of SCO systems were calculated based on anisotropic sphere model describing the volume and shape changes of the lattice at the transition [68–70]. Though the anisotropic models were found to describe the spin crossover phenomena successfully, these models have not been very successful in describing the cooperativity with the exception of a recent work by Spiering et al. [70] where transitions both with and without hysteresis have been achieved. In the model by Spiering et al. [70], an anharmonic lattice having SCO molecules having a certain misfit to the lattice was considered, which were assumed to interact via elastic interactions by the change of shape and volume.

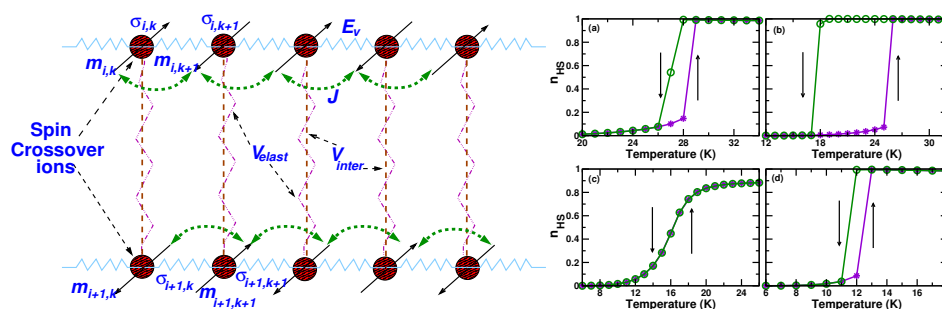


Figure 4. Figure showing schematic diagram of various interactions present in linear SCO polymeric systems along with their respective effects on the system. The left panel shows all the interactions present in the system. The red balls denote the SCO ions. The light blue springs denote the intra chain spin dependent elastic interaction. The black arrows denote the magnetic spins at the SCO sites with the green bent arrows denoting the magnetic exchange between the spins. The pink dashed lines show the inter chain elastic interaction and the brown dashed lines show the interchain superexchange interaction. The right panel shows 4 different graphs showing the effect of (a) ferroelastic intra chain interaction in absence of magnetic interaction (b) ferroelastic in presence of magnetic intra chain interaction (c) anti ferroelastic intra chain interaction in absence of magnetic interaction and (d) anti-ferroelastic in presence of magnetic intra chain interaction. Figure has been adapted from Banerjee et al. [71].

The above described approaches of considering the elastic interaction as the sole driving mechanism, however completely disregards the importance of the long range magnetic interaction that may build up between transition metal centers via superexchange interaction mediated through the organic linkers connecting the metal centers. In order to address this issue, in the study by Timm [72], the collective properties of spin-crossover chains were investigated taking into account both elastic interaction and Ising-like magnetic interaction, and the ground state phase diagram was mapped out. This calculation though ignored the spin-phonon coupling, considering the elastic interactions to be spin independent, and thus were unable to distinguish between ferro and antiferroelastic situations. In a recent study, Banerjee et al. [71] have studied extensively the microscopic mechanism giving rise to cooperativity in spin crossover considering both the effect of magnetic super-exchange interaction and elastic interactions together with spin-phonon coupling in a coupled 1-d chain model. A model Hamiltonian was setup in the basis of pseudo-spins, corresponding to the elastic part of the interaction, and the actual spin quantum number, describing the magnetic superexchange interaction. The system consisted of connected chains of spin-crossover ions, as shown in left panel of Figure 4. The SCO ions in a chain were assumed to be connected by intrachain elastic interactions that depend on their spin states given by $E_v(\sigma_{i,k}, \sigma_{i,k+1})$, where σ denotes fictitious spins or pseudo spins as described above, and $E_v(\sigma_{i,k}, \sigma_{i,k+1}) = \frac{e_{k,k+1}}{2} q_i^2$ wherein q_i denotes the small displacements. The spin dependence of $e_{k,k+1}$ was considered to be same as in the model by Boukheddaden et al. [67]. Magnetism was accounted for by actual spin S , where $m_{i,k} = S_{i,k}$ with $m_{i,k} = 0$ for $\sigma_{i,k} = -1$ (LS state) and $m_{i,k} = -2, \dots, 2$ for $\sigma_{i,k} = 1$, corresponding to the HS state $S = 2$. Thus the constructed model Hamiltonian was given by,

$$\mathcal{H} = - \sum_k E_v \sigma_{i,k} \sigma_{i,k+1} + \Delta \sum_{i,k} \sigma_{i,k} + J \sum_k m_{i,k} m_{i,k+1} \\ + \sum_{i \neq k} [V_{\perp} \sigma_{i,k} \sigma_{i+1,k} + V_{\parallel} (\sigma_{i,k} + \sigma_{i+1,k})]$$

where Δ denoted the difference in energy between the HS and the LS states, V_{\perp} and V_{\parallel} represented the interchain interactions arising out of electrostatic and steric interactions, respectively, as discussed earlier. The third term of the Hamiltonian describes the magnetic exchange, which involves Ising-like antiferromagnetic superexchange interaction J acting between two Fe^{2+} ions with spin $S = 2$.

The Monte Carlo study of this above model Hamiltonian established the important role of magnetic super-exchange interaction acting between the SCO ions, in the cooperativity of the spin transition. They turn out to be equally important as the elastic interaction. Depending on the nature of the spin-dependent elastic interaction, which depends on the nature of the spin-phonon coupling, the magnetic super-exchange was found to contribute in development of cooperativity in a quantitative or qualitative manner. In case of ferrottype elastic interaction, the super-exchange interaction was found to enhance the hysteresis effect, setup by the elastic interaction. In the case of antiferro nature of elastic interaction, the magnetic exchange interaction was found to play a decisive role in driving the hysteresis in the system, putting the elastic coupling to a back seat. As is seen from the right panel of Figure 4 in presence of antiferro type intra chain elastic interaction alone, the system did not show any hysteresis. Only when the magnetic superexchange interaction J was introduced, a hysteresis loop was observed in the HS fraction. It was thus concluded that the magnetic superexchange interaction is of prime importance in driving cooperativity in the system if the intra chain elastic interaction is of antiferro type.

In another study a vibronic model for the SCO transition has been proposed [73], where the coupling between spin state and molecular geometry was considered, which causes quantum mixing between LS and HS states resulting from higher order spin-orbit coupling. It was concluded from such study that non-adiabaticity does not play an important role in case of cooperativity.

4. Ab Initio Studies on Materials Showing Cooperativity

These materials of technological importance, however, are challenges for material specific, predictive theoretical descriptions through ab-initio calculations. Challenges arise due to (a) strong electron-electron correlation in open *d* shell of the transition metal SCO centers; (b) complex geometry of the materials with large number of atoms in the unit cell; and (c) externally stimulated changes in electronic and structural properties. Both wavefunction based quantum chemical approaches [74–79] and density based Density functional theory (DFT) [80–83] calculations have been undertaken to study the phenomena of SCO in general. However it appears that the wavefunction based approaches require quite a large basis set and even though various techniques like complete active space self-consistent field (CASSCF) [75] or CASPT2 method [76], the coupled-cluster (CC) theory or its variation CCSD(T) method [79], (S and D denote inclusion of single and double excitations, respectively and (T) represents a single/triple correct term) have been used, these methods are computationally quite expensive and application of these methods to 2 or 3 dimensional connectivity of metal–organic frameworks is not feasible. We shall thus primarily discuss and describe applications of DFT based methods which have been used to study the cooperativity in SCO systems. The DFT based methods can handle a large number of atoms in the periodic systems quite efficiently, and can also take advantage of DFT+U methods [84] with supplemented onsite Hubbard U parameter to handle strong correlation effect at transition metal sites. As established, the influence of external perturbation like pressure on crystal structure and electronic structure can be described rather accurately through DFT calculations. Therefore, DFT calculations incorporate the metal-ligand bond length change that happens during SCO, which has been pointed out as an important ingredient driving SCO [85]. The handling of temperature effect within DFT is more challenging which is achievable in recent time through the progress made in ab-initio molecular dynamics (AIMD) simulations [86]. AIMD simulations solve electronic Kohn–Sham equation and Newton’s equation of motion for ions, coupled via Hellmann-Feynmann theorem for forces. In the following we describe in detail application of such state-of-art techniques to two representative cases, one of linear coordination polymer and another of hybrid perovskite. There also exists two other DFT studies, cyanide-based bimetallic 3-d coordination polymers [81,83]. The study by Tarafder et al. [83] also studied the hysteresis effect in the pressured induced spin state transitions in cyanide-based Fe–Nb 3-d coordination polymer.

4.1. Linear or 1-d Coordination Polymers

Considering the example of a linear coordination polymeric compound, Fe-triazole complex, the existence of hysteresis through ab initio molecular dynamics (AIMD) simulation was shown in a recent study by Banerjee et al. [71] As shown in left panel of Figure 5, a simple computer designed model of Fe-triazole complex like $\text{Fe}[(\text{hyetrz})_3](4\text{-chlorophenylsulphonate})_2 \cdot 3\text{H}_2\text{O}$ where hyetrz stands for 4-(2'-hydroxyethyl)-1,2,4-triazole was considered in this study. The polymeric Fe(II) triazole compound mentioned above, consists of Fe(II) ions with neighboring iron ions connected through three pyrazole bridges, forming a chain like structure where the counterions and non bonded water molecules form the links between the chains. Even though this compound shows SCO with associated hysteresis, there is hardly any available crystal structure, owing to the fact that the samples were only available in the form of powder, insoluble in water and organic solvents. Absence of accurate crystal structure data pose a problem for computational study. The SCO property in Fe-triazole compounds has been seen for variety of choices of counterions and the residues. A simplified model crystal structure was thus used in the study by Banerjee et al. [71], where the local environment around Fe(II) ions was kept same as in real compounds, and the distant environment was simplified to a large extend. In the simplified model the counterions were replaced by F^- with the substituent being chosen as CH_3 and non-bonded water molecules were removed for the sake of simplification (cf. top panel of Figure 5).

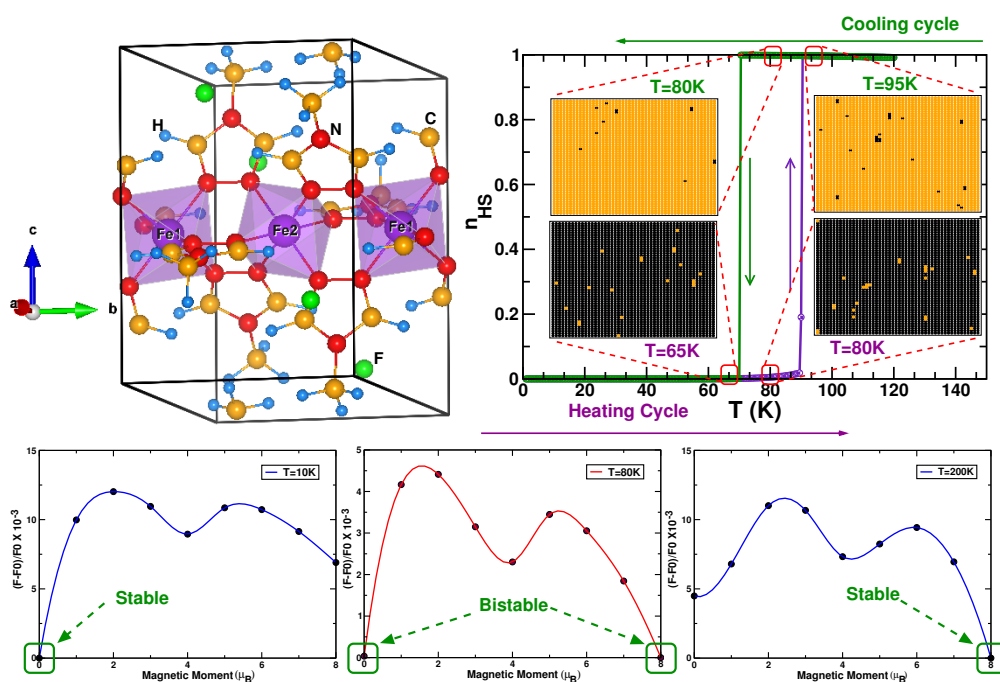


Figure 5. Figure showing crystal structure of Fe-triazole complex along with AIMD and DFT based model Hamiltonian MC study on Fe-triazole. The top left panel shows the simplified computer designed model of $\text{Fe}[(\text{hyetrz})_3](4\text{-chlorophenylsulphonate})_2 \cdot 3\text{H}_2\text{O}$. The medium sized golden and red balls represent N and C, respectively. The small sky blue balls represent the H atoms, while the green medium sized balls denote counterion F^- . The top right panel shows HS fraction as a function of increasing and decreasing temperature, as given in MC study with DFT based elastic and magnetic interactions. The insets are the snapshots of pseudo-spin configurations in a 50×50 lattice with LS(HS) state shown in black (yellow), at $T = 65$ K and 80 K in the heating cycle and at 80 K and 95 K in the cooling cycle. At $T = 80$ K, in the HS and LS states are seen to coexist demonstrating the bistability in the system. The bottom panel shows the free energy profiles at three different temperatures $T = 10$ K, 80 K, and 200 K. Figure has been adapted from Banerjee et al. [71].

The AIMD calculations were carried out within the framework of DFT implemented on a plane wave basis set in Vienna Ab-initio Simulation package (VASP) [87]. The exchange correlation functional was approximated by Perdew-Burke-Ernzerhof [88] (PBE)+U functional. In contrast to classical molecular dynamics where the ground state potential energy surface is represented in the force field, in case of Ab initio molecular dynamics the electronic behavior is obtained in a first principles manner by using a quantum mechanical method, like DFT as is the case under discussion. Born-Oppenheimer AIMD was carried out which is a MD on a Born-Oppenheimer surface. Calculations were carried out using the canonical ensemble and a thermostat was used to exchange the energy of endothermic and exothermic processes. Corresponding to the thermal expansion of Fe-triazole at the various studied temperatures the atomic positions were relaxed at 0 K at various chosen volumes, until the maximum forces on atoms were less than $0.01 \text{ eV}/\text{\AA}^0$. The temperature was then increased within the NVT ensemble from $T = 0$ K to the desired final temperature using a Berendsen thermostat with a time step of 1 fs for each MD step. At the final step the system was thermalized for a time duration of 1 ps using the Nosé-Hoover thermostat. At the very end, a microcanonical NVE ensemble thermalization was carried out to evaluate the free energy of the system at the final temperature.

The AIMD calculations were carried out at temperatures of 10 K, 80 K, and 200 K, the choice of temperatures being dictated by the experimental measure of susceptibility on Fe-triazole, [82] for which a transition is found to occur at ~ 80 K with a hysteresis width of ~ 20 K. Free energy profiles were created by plotting the Free energy as a function of the fixed magnetic moments and it was

observed that for 10 K the LS state $S = 0$ was the lowest energy state while for 200 K the HS state was the lowest energy state with $S = 2$. However a clear bistability was observed at 80 K (cf. bottom panel in Figure 5) proving the capability of the method to capture the cooperativity developed in the system.

Obtaining the intra chain elastic interaction parameters were shown to be imperative in case of Fe-triazole since it is the combination of intra chain elastic parameters that determines whether the effective elastic interaction is ferro- or antiferro- type. In this case the spin dependent intra chain elastic interactions, as defined in the previous section setting the small displacement $q = 0.005$ turn out to be as follows: $E_{v(++)} = 72$ K, $E_{v(--)} = 101$ K, and $E_{v(+-)} = 80$ K. This clearly shows that the intra chain elastic interaction is of antiferro type. It was thus inferred that the observed bistability and consequently hysteresis in this linear polymeric SOC system is driven by the magnetic exchange interaction.

In a previous work by Jeschke et al. [82] the magnetic exchanges in Fe-triazole complex was computed from DFT. This paper is particularly notable since from ab-initio perspective, this was first study to point out that magnetic exchange might be as important as elastic interaction in giving rise to the cooperativity in these compounds. The magnetic superexchange interactions between neighboring Fe ions were calculated by carrying out DFT+U total energy calculations of FM and AFM orientations of Fe spins considering the predominance of the HS states between the ions. The energy difference between the two spin orientations gave rise to a antiferromagnetic superexchange interaction of magnitude 18 K.

Plugging in the DFT estimated values of material specific constants with good approximations for parameters like Δ which are not easy to calculate using DFT methods, MC simulations on first-principles derived model Hamiltonian carried out by Banerjee et al. [71]. The results are shown in the top right panel of Figure 5. The calculated LS-HS transition temperature was found to be $T_C = 80$ K with the large hysteresis, and the width of the hysteresis was found to be $\Delta T = 20$ K, both in excellent agreement with that obtained from the measured susceptibility reported for the real compound, [82] proving the effectiveness of first-principles approach. Top right panel of Figure 5, also shows the snapshots of the pseudo-spin configurations of the lattice at different temperatures, $T < T_C$, $T > T_C$ and $T = T_C$ during the heating and the cooling cycles of the MC simulation. The snapshot configuration of pseudo-spins at $T = T_C$ show sites with primarily HS configurations for the cooling cycle and LS configurations for the heating cycle, establishing signature of bistability in this material, in conformity with the results obtained from rigorous AIMD simulations.

4.2. Hybrid Perovskites

While the hybrid perovskites have been discussed heavily in literature for many different potential applications, as discussed in introduction, they have not been explored as possible SCO materials. The pressure-driven cooperative spin crossover in metal-organic hybrid perovskites, apparently unconventional materials for SCO, was proposed and investigated by Banerjee et al. [46] using DFT based electronic structure calculations. By considering two popular hybrid perovskite materials, viz., Dimethylammonium Iron Formate (DMAFeF) and Hydroxylamine Iron Formate (HAFef), [46] crystal structures of which are shown in the left panel of Figure 6, it was demonstrated that application of external pressure can drive spin state transition along with associated hysteresis in these compounds. Interestingly the width of hysteresis turned out to be rather different for the two compounds with two different cations DMA and HA, indicating possible tuning of cooperativity by chemical means.

The mechanical strengths of DMAFeF and HAFef were calculated using DFT+U calculations in plane wave basis to understand the microscopic origin of the quantitative differences in response to the applied pressure of the two perovskite hybrids. It was argued that due to the very different strength and number of H bonding in the two compounds, the lattice for HAFef is more rigid compared to that of DMAFeF. The difference in the H bondings in the two cases was understood in terms of enhanced polarity of O-H bond compared to the N-H bond due to the differences in electronegativity of N and O with O being more electronegative compared to N. The magnitudes of the calculated bulk moduli of the two systems confirmed this fact. The bulk modulus turned out to be 21.55 GPa for DMAFeF and

24.27 GPa for HAFeF respectively. The critical pressure required to induce spin-switching through change in Fe–O bond-length was found to be significantly larger in more rigid lattice of HAFeF compared to that in less rigid lattice of DMAFeF. This was reflected in different values of $P_{C\uparrow}$ (critical pressure in increasing pressure path) in the two compounds as seen from Figure 6. A significant hysteresis was found in both compounds in terms of differences between $P_{C\uparrow}$ and $P_{C\downarrow}$ (critical pressure in increasing and decreasing pressure path, respectively).

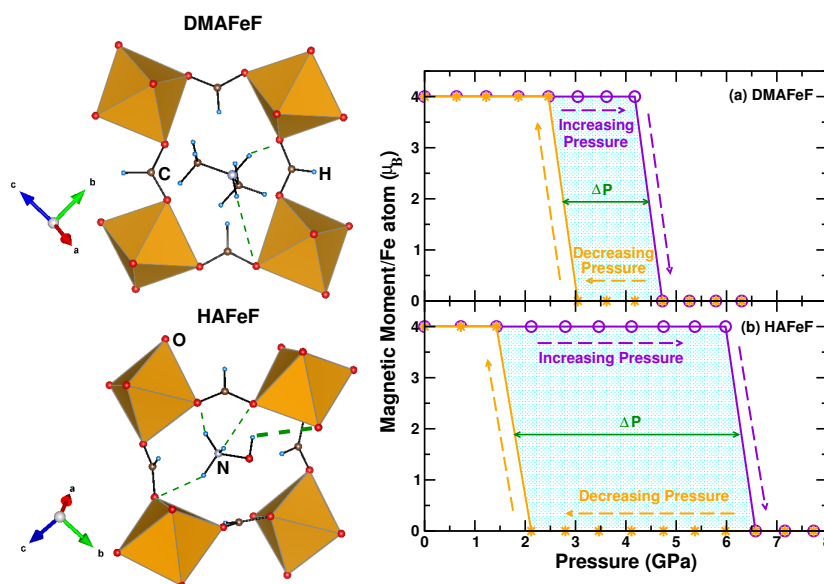


Figure 6. Figure showing the effect of exerting and releasing pressure on DMAFeF and HAFeF. The **left** panel shows the crystal structures of DMAFeF and HAFeF. In the crystal structure the golden octahedra denote the Fe–O octahedra. C, N, H and O are marked in the figure. The N–H ··· O H bonding is marked with a thin dashed green line whereas the O–H ··· O H bonding is marked with a thick dashed green line to show the relative difference of their strengths arising due to the difference in polarity of N–H and O–H bonds; The **right** panel shows comparatively the plots of Magnetic Moment/Fe atom as a function of pressure for both DMAFeF (**top**) and HAFeF (**bottom**). Figure has been adapted from Banerjee et al. [46].

As discussed in Section 3, the interplay between elastic and magnetic interaction in building up cooperativity relies significantly on the spin-dependent rigidity of the lattice. In the study by Banerjee et al. [46] the authors found DMAFeF to be very weakly ferroelastic with $e_{+-} \simeq \sqrt{e_{++}e_{--}}$ while HAFeF was found to be strongly ferroelastic with $e_{+-} > \sqrt{e_{++}e_{--}}$. The effective elastic constants for DMAFeF and HAFeF were found to be 3.52 K and 8.93 K respectively thus making it evident that the contribution to cooperativity and hence the enhanced hysteresis width in HAFeF comes primarily from elastic interaction. The calculated magnetic superexchanges turned out to be of similar values for DMAFeF and HAFeF (3.19 K and 2.85 K) and negative indicating antiferromagnetic nature of magnetic exchanges. This lead to the conclusion that while the magnetic exchanges in the two compounds are of same sign and similar strengths, the spin-dependent elastic interactions are of ferroelastic nature with significantly larger strength for HAFeF compared to DMAFeF. The latter is responsible for HAFeF having a sufficiently larger hysteresis loop width compared to DMAFeF. It was thus concluded that the primary factor responsible in driving cooperativity in these formate frameworks is the spin-dependent lattice effect, which gets assisted by the magnetic exchange. This aspect in hybrid perovskites is very different from the previously described case of linear coordination polymers in which magnetic superexchange was found to have a dominating effect on cooperativity.

5. Summary and Outlook

In this review, we focused on the issue of cooperativity in SCO properties exhibited by coordination polymers with extended solid state structures, as in linear coordination polymers, or hybrid perovskites. This topic needs attention from the perspective of understanding of microscopic mechanisms driving cooperativity, and the use of the obtained understanding in designing of suitable materials aimed at improving the performance of the devices based on them. In this article, we have discussed different model studies proposed for microscopic understanding of cooperativity. Out of these studies, it emerged that the cooperativity-assisted hysteresis is primarily driven by magnetic super-exchanges in case of systems with elastic interactions of antiferroelastic type. In case of systems described by ferroelastic interactions, on the other hand, it is the elastic interaction that builds up the cooperativity-assisted hysteresis with magnetic super-exchange playing a secondary role. It was further demonstrated through rigorous first-principles calculations, considering specific examples, that while the chain polymeric compounds with SCO centers connected by chemical bonds belong to first category, the hybrid perovskites where H-bondings are important belong to the second category. We would like to stress at this point that the work described here on hybrid perovskites is theoretical proposal for which experimental validation needs to be carried out. So far this has remained as an unexplored territory for hybrid perovskites which deserves attention.

This review focused solely on theoretical studies of temperature and pressure induced cooperative SCO. A much less studied and worth exploring area from theoretical point of view would be study of cooperativity in light induced spin state trapping. While empirical theories have been proposed within the non-adiabatic multiphonon framework [89] for mononuclear compounds in terms of ΔE_{HL}^0 , the energy difference between the lowest vibrational levels of HS and LS states, and the change of metal–ligand bond length Δr_{HL} , the ab-initio description of the complete process is lacking, apart from few quantum-chemical calculations [90,91] studying the electronic structure of excited state geometries. More importantly, extension to multinuclear systems with possible cooperative effect is non-existent. The study by Létard et al. [61] through irradiation of the sample at low temperature with laser coupled to an optical fiber within a SQUID cavity showed that the temperature dependence of the photomagnetic properties of mononuclear and multinuclear systems to be very different. To the best of our knowledge no microscopic theory has been developed to explain this difference.

This review also focused on Fe(II) based systems, which are so far the most popular ones. However, in addition to Fe or Co based systems, there are few examples of SCO in Mn(III) [92,93]. Mn(III) is a particularly interesting candidate for SCO as it should exhibit a significant Jahn–Teller effect in its HS state. It is an interesting question to ask how the Jahn–Teller distortion effects lattice contribution to cooperativity in terms of influencing the spin-lattice coupling. This may result into different profiles of SCO, like double transition, compared to those observed for Fe(II). This issue demands future attention.

Finally, hybrid perovskites which are the new candidates proposed for observing cooperative SCO effect, should be also explored for LIESST effect both from experimental and theoretical point of view. Given the observation of multiferroicity, already reported in literature for hybrid perovskites, it will be also worth to investigate any exotic magnetic ordering of HS Fe(II)'s leading to breaking of inversion symmetry, and thus resulting into magneto-electric coupling.

Acknowledgments: Hrishit Banerjee and Tanusri Saha-Dasgupta acknowledge the support of Department of Science and Technology (DST) India, Nanomission for funding through Thematic Unit of Excellence on Computational Materials Science.

Author Contributions: The literature survey was carried out by Hrishit Banerjee and Sudip Chakraborty. The manuscript was written by Hrishit Banerjee and Tanusri Saha-Dasgupta. The project was coordinated by Tanusri Saha-Dasgupta.

Conflicts of Interest: The authors declare no conflict of interest.

Abbreviations

The following abbreviations are used in this manuscript:

SCO	Spin crossover
MOF	Metal organic framework
LS	Low Spin
HS	High Spin
EXAFS	Extended X-ray absorption Fine Structure
FT-IR	Fourier Transform Infrared Spectroscopy
UV-vis	Ultraviolet and visible
EPR	Electron Paramagnetic Resonance
μ SR	Muon Spin Relaxation
PAS	Positron Annihilation Spectroscopy
NRS	Nuclear Resonant Scattering of synchrotron radiation
LIESST	Light induced spin state trapping
SQUID	Superconducting quantum interference device
trz	triazole
btr	bis-triazole
bipy	4,4'-bipyridine
bpea	1,2-bis(4-pyridyl)ethane
bppa	1,3-bis(4-pyridyl)propane
hyetrz	4-(2'-hydroxyethyl)-1,2,4-triazole
MC	Monte Carlo
DFT	Density functional theory
CASSCF	Complete active space self consistent field
CASPT2	Complete active space with second order perturbation theory
CC	Couple cluster theory
CCSD(T)	Coupled Cluster single-double and perturbative triple
VASP	Vienna Ab-initio Simulation Package
PBE	Perdew, Burke and Ernzerhof
AIMD	Ab-initio Molecular dynamics
DMAFeF	Dimethyl ammonium Iron Formate
HAFeF	Hydroxyl ammonium Iron Formate

References

1. Létard, J.-F.; Guionneau, P.; Goux-Capes, L. *Spin Crossover in Transition Metal Compounds I-III*; Gütllich, P., Goodwinpp, H., Eds.; Springer: Berlin, Germany, 2004; pp. 221–249.
2. Linares, J.; Codjovi, E.; Garcia, Y. Pressure and Temperature Spin Crossover Sensors with Optical Detection. *Sensors* **2012**, *12*, 4479–4492.
3. Cobo, S.; Molnár, G.; Real, J.A.; Bousseksou, A. Multilayer Sequential Assembly of Thin Films that Display Room-Temperature Spin Crossover with Hysteresis. *Angew. Chem. Int. Ed.* **2006**, *45*, 5786–5789.
4. Saha-Dasgupta, T.; Oppeneer, P.M. Computational design of magnetic metal–organic complexes and coordination polymers with spin-switchable functionalities. *MRS Bull.* **2014**, *39*, 614–620.
5. Brooker, S.; Kitchen, J.A. Nano-magnetic materials: Spin crossover compounds vs. single molecule magnets vs. single chain magnets. *Dalton Trans.* **2009**, 7331–7340, doi:10.1039/B907682D.
6. Ohkoshi, S.I.; Imoto, K.; Tsunobuchi, Y.; Takano, S.; Tokoro, H. Light-induced spin-crossover magnet. *Nat. Chem.* **2011**, *3*, 564–569.
7. Halder, G.J.; Kepert, C.J.; Moubaraki, B.; Murray, K.S.; Cashion, J.D. Guest-Dependent Spin Crossover in a Nanoporous Molecular Framework Material. *Science* **2002**, *298*, 1762–1765.
8. Olguín, J.; Brooker, S. Spin crossover active iron(II) complexes of selected pyrazole-pyridine/pyrazine ligands. *Coord. Chem. Rev.* **2011**, *255*, 203–240.

9. Batten, S.R.; Champness, N.R.; Chen, X.M.; Garcia-Martinez, J.; Kitagawa, S.; Öhrström, L.; O’Keeffe, M.; Suh, M.P.; Reedijk, J. Terminology of metal–organic frameworks and coordination polymers (IUPAC Recommendations 2013). *Pure Appl. Chem.* **2013**, *85*, 1715–1724.
10. Ozarowski, A.; Shunzhong, Y.; McGarvey, B.R.; Mislankar, A.; Drake, J.E. EPR and NMR study of the spin-crossover transition in bis(4,4’-bi-1,2,4-triazole)bis(thiocyanato)iron hydrate and bis(4,4’-bi-1,2,4-triazole)bis(selenocyanato)iron hydrate. X-ray structure determination of Fe(4,4’-bi-1,2,4-triazole)₂(SeCN)₂·H₂O. *Inorg. Chem.* **1991**, *30*, 3167–3174, doi:10.1021/ic00016a013.
11. Yann Garcia, N.N.A.; Naik, A.D. Crystal Engineering of Fe-II Spin Crossover Coordination Polymers Derived from Triazole or Tetrazole Ligands. *Chimia* **2013**, *67*, 411–418, doi:10.2533/chimia.2013.411.
12. Morris, R.; Wheatley, P. Gas Storage in Nanoporous Materials. *Angew. Chem. Int. Ed.* **2008**, *47*, 4966–4981.
13. Kreno, L.E.; Leong, K.; Farha, O.K.; Allendorf, M.; Van Duyne, R.P.; Hupp, J.T. Metal–Organic Framework Materials as Chemical Sensors. *Chem. Rev.* **2012**, *112*, 1105–1125, doi:10.1021/cr200324t, PMID:22070233.
14. Horcajada, P.; Chalati, T.; Serre, C.; Gillet, B.; Sebrie, C.; Baati, T.; Eubank, J.F.; Heurtaux, D.; Clayette, P.; Kreuz, C.; et al. Porous metal–organic-framework nanoscale carriers as a potential platform for drug delivery and imaging. *Nat. Mater.* **2010**, *9*, 172–178.
15. Czaja, A.U.; Trukhan, N.; Muller, U. Industrial applications of metal–organic frameworks. *Chem. Soc. Rev.* **2009**, *38*, 1284–1293.
16. Cheetham, A.K.; Rao, C.N.R. There’s Room in the Middle. *Science* **2007**, *318*, 58–59.
17. Garcia, Y.; Niel, V.; Muñoz, M.C.; Real, J.A. Spin Crossover in 1D, 2D and 3D Polymeric Fe(II) Networks. In *Spin Crossover in Transition Metal Compounds I*; Gütllich, P., Goodwin, H., Eds.; Springer: Berlin/Heidelberg, Germany, 2004; pp. 229–257.
18. Krober, J.; Codjovi, E.; Kahn, O.; Groliere, F.; Jay, C. A spin transition system with a thermal hysteresis at room temperature. *J. Am. Chem. Soc.* **1993**, *115*, 9810–9811, doi:10.1021/ja00074a062.
19. Setifi, F.; Milin, E.; Charles, C.; Thétiot, F.; Triki, S.; Gómez-García, C.J. Spin Crossover Iron(II) Coordination Polymer Chains: Syntheses, Structures, and Magnetic Characterizations of [Fe(aqin)₂(μ₂-M(CN)₄)] (M = Ni(II), Pt(II), aqin = Quinolin-8-amine). *Inorg. Chem.* **2014**, *53*, 97–104, doi:10.1021/ic401721x.
20. Schonfeld, S.; Lochenie, C.; Thoma, P.; Weber, B. 1D iron(II) spin crossover coordination polymers with 3,3[prime or minute]-azopyridine-kinetic trapping effects and spin transition above room temperature. *CrystEngComm* **2015**, *17*, 5389–5395.
21. Bauer, W.; Lochenie, C.; Weber, B. Synthesis and characterization of 1D iron(II) spin crossover coordination polymers with hysteresis. *Dalton Trans.* **2014**, *43*, 1990–1999.
22. Manser, J.S.; Christians, J.A.; Kamat, P.V. Intriguing Optoelectronic Properties of Metal Halide Perovskites. *Chem. Rev.* **2016**, *116*, 12956–13008, doi:10.1021/acs.chemrev.6b00136, PMID:27327168.
23. Mitzi, D.B.; Feild, C.A.; Harrison, W.T.A.; Guloy, A.M. Conducting tin halides with a layered organic-based perovskite structure. *Nature* **1994**, *369*, 467–469.
24. Náfrádi, B.; Szirmai, P.; Spina, M.; Lee, H.; Yazyev, O.V.; Arakcheeva, A.; Chernyshov, D.; Gibert, M.; Forró, L.; Horváth, E. Optically switched magnetism in photovoltaic perovskite CH₃NH₃(Mn:Pb)I₃. *Nat. Commun.* **2016**, *7*, 13406.
25. Kojima, A.; Teshima, K.; Shirai, Y.; Miyasaka, T. Organometal Halide Perovskites as Visible-Light Sensitizers for Photovoltaic Cells. *J. Am. Chem. Soc.* **2009**, *131*, 6050–6051, doi:10.1021/ja809598r, PMID:19366264.
26. Zhou, H.; Chen, Q.; Li, G.; Luo, S.; Song, T.B.; Duan, H.S.; Hong, Z.; You, J.; Liu, Y.; Yang, Y. Interface engineering of highly efficient perovskite solar cells. *Science* **2014**, *345*, 542–546.
27. Heo, J.H.; Song, D.H.; Han, H.J.; Kim, S.Y.; Kim, J.H.; Kim, D.; Shin, H.W.; Ahn, T.K.; Wolf, C.; Lee, T.W.; et al. Planar CH₃NH₃PbI₃ Perovskite Solar Cells with Constant 17.2% Average Power Conversion Efficiency Irrespective of the Scan Rate. *Adv. Mater.* **2015**, *27*, 3424–3430.
28. Burschka, J.; Pellet, N.; Moon, S.J.; Humphry-Baker, R.; Gao, P.; Nazeeruddin, M.K.; Gratzel, M. Sequential deposition as a route to high-performance perovskite-sensitized solar cells. *Nature* **2013**, *499*, 316–319.
29. Liu, M.; Johnston, M.B.; Snaith, H.J. Efficient planar heterojunction perovskite solar cells by vapour deposition. *Nature* **2013**, *501*, 395–398.
30. Wang, Z.; Hu, K.; Gao, S.; Kobayashi, H. Formate-Based Magnetic Metal–Organic Frameworks Templated by Protonated Amines. *Adv. Mater.* **2010**, *22*, 1526–1533.

31. Jain, P.; Dalal, N.S.; Toby, B.H.; Kroto, H.W.; Cheetham, A.K. Order-Disorder Antiferroelectric Phase Transition in a Hybrid Inorganic–Organic Framework with the Perovskite Architecture. *J. Am. Chem. Soc.* **2008**, *130*, 10450–10451, doi:10.1021/ja801952e, PMID:18636729.
32. Jain, P.; Ramachandran, V.; Clark, R.J.; Zhou, H.D.; Toby, B.H.; Dalal, N.S.; Kroto, H.W.; Cheetham, A.K. Multiferroic Behavior Associated with an Order-Disorder Hydrogen Bonding Transition in Metal–Organic Frameworks (MOFs) with the Perovskite ABX₃ Architecture. *J. Am. Chem. Soc.* **2009**, *131*, 13625–13627, doi:10.1021/ja904156s, PMID:19725496.
33. Weng, D.F.; Wang, Z.M.; Gao, S. Framework-structured weak ferromagnets. *Chem. Soc. Rev.* **2011**, *40*, 3157–3181.
34. Stroppa, A.; Jain, P.; Barone, P.; Marsman, M.; Perez-Mato, J.M.; Cheetham, A.K.; Kroto, H.W.; Picozzi, S. Electric Control of Magnetization and Interplay between Orbital Ordering and Ferroelectricity in a Multiferroic Metal–Organic Framework. *Angew. Chem. Int. Ed.* **2011**, *50*, 5847–5850.
35. Di Sante, D.; Stroppa, A.; Jain, P.; Picozzi, S. Tuning the Ferroelectric Polarization in a Multiferroic Metal–Organic Framework. *J. Am. Chem. Soc.* **2013**, *135*, 18126–18130, doi:10.1021/ja408283a, PMID:24191632.
36. Stroppa, A.; Barone, P.; Jain, P.; Perez-Mato, J.M.; Picozzi, S. Hybrid Improper Ferroelectricity in a Multiferroic and Magnetoelectric Metal–Organic Framework. *Adv. Mater.* **2013**, *25*, 2284–2290.
37. Jain, P.; Stroppa, A.; Nabok, D.; Marino, A.; Rubano, A.; Paparo, D.; Matsubara, M.; Nakotte, H.; Fiebig, M.; Picozzi, S.; et al. Switchable electric polarization and ferroelectric domains in a metal–organic-framework. *Npj Quant. Mater.* **2016**, *1*, 16012.
38. Tian, Y.; Stroppa, A.; Chai, Y.; Yan, L.; Wang, S.; Barone, P.; Picozzi, S.; Sun, Y. Cross coupling between electric and magnetic orders in a multiferroic metal–organic framework. *Sci. Rep.* **2014**, *4*, 6062.
39. Tian, Y.; Stroppa, A.; Chai, Y.S.; Barone, P.; Perez-Mato, M.; Picozzi, S.; Sun, Y. High-temperature ferroelectricity and strong magnetoelectric effects in a hybrid organic–inorganic perovskite framework. *Phys. Status Solidi Rapid Res. Lett.* **2015**, *9*, 62–67.
40. Zhao, W.P.; Shi, C.; Stroppa, A.; Di Sante, D.; Cimpoesu, F.; Zhang, W. Lone-Pair-Electron-Driven Ionic Displacements in a Ferroelectric Metal–Organic Hybrid. *Inorg. Chem.* **2016**, *55*, 10337–10342, doi:10.1021/acs.inorgchem.6b01545, PMID:27676140.
41. Gómez-Aguirre, L.C.; Pato-Doldán, B.; Stroppa, A.; Yáñez-Vilar, S.; Bayarjargal, L.; Winkler, B.; Castro-García, S.; Mira, J.; Sánchez-Andújar, M.; Señaris-Rodríguez, M.A. Room-Temperature Polar Order in [NH₄][Cd(HCOO)₃]*—*A Hybrid Inorganic–Organic Compound with a Unique Perovskite Architecture. *Inorg. Chem.* **2015**, *54*, 2109–2116, doi:10.1021/ic502218n, PMID:25664382.
42. Kamminga, M.E.; Stroppa, A.; Picozzi, S.; Chislov, M.; Zvereva, I.A.; Baas, J.; Meetsma, A.; Blake, G.R.; Palstra, T.T.M. Polar Nature of (CH₃NH₃)₃Bi₂I₉ Perovskite-Like Hybrids. *Inorg. Chem.* **2017**, *56*, 33–41, doi:10.1021/acs.inorgchem.6b01699, PMID:27626290.
43. Ptak, M.; Maczka, M.; Gagor, A.; Sieradzki, A.; Stroppa, A.; Di Sante, D.; Perez-Mato, J.M.; Macalik, L. Experimental and theoretical studies of structural phase transition in a novel polar perovskite-like [C₂H₅NH₃][Na_{0.5}Fe_{0.5}(HCOO)₃] formate. *Dalton Trans.* **2016**, *45*, 2574–2583.
44. Ghosh, S.; Di Sante, D.; Stroppa, A. Strain Tuning of Ferroelectric Polarization in Hybrid Organic Inorganic Perovskite Compounds. *J. Phys. Chem. Lett.* **2015**, *6*, 4553–4559, doi:10.1021/acs.jpcclett.5b01806, PMID:26512946.
45. Mazzuca, L.; Cañadillas-Delgado, L.; Rodríguez-Velamazán, J.A.; Fabelo, O.; Scarrozza, M.; Stroppa, A.; Picozzi, S.; Zhao, J.P.; Bu, X.H.; Rodríguez-Carvajal, J. Magnetic Structures of Heterometallic M(II)–M(III) Formate Compounds. *Inorg. Chem.* **2017**, *56*, 197–207, doi:10.1021/acs.inorgchem.6b01866, PMID:27935298.
46. Banerjee, H.; Chakraborty, S.; Saha-Dasgupta, T. Cationic Effect on Pressure Driven Spin-State Transition and Cooperativity in Hybrid Perovskites. *Chem. Mater.* **2016**, *28*, 8379–8384, doi:10.1021/acs.chemmater.6b03755.
47. Cambi, L.; Szegő, L. Über die magnetische Suszeptibilität der komplexen Verbindungen. *Berichte der Deutschen Chemischen Gesellschaft (A B Ser.)* **1931**, *64*, 2591–2598.
48. Stouffer, R.C.; Busch, D.H.; Hadley, W.B. Unusual Magnetic Properties of Some Six-Coördinate Cobalt(II) Complexes 1—Electronic Isomers. *J. Am. Chem. Soc.* **1961**, *83*, 3732–3734, doi:10.1021/ja01478a051.
49. Madeja, K.; König, E. Zur frage der bindungsverhältnisse in komplexverbindungen des eisen(II) mit 1,10-phenanthrolin. *J. Inorg. Nucl. Chem.* **1963**, *25*, 377–385.
50. Kojima, N.; Murakami, Y.; Komatsu, T.; Yokoyama, T. EXAFS study on the spin-crossover system, [Fe(4-NH₂trz)₃](R-SO₃)₂. *Synth. Met.* **1999**, *103*, 2154.

51. Okabayashi, J.; Ueno, S.; Wakisaka, Y.; Kitazawa, T. Temperature-dependent EXAFS study for spin crossover complex: $\text{Fe}(\text{pyridine})_2\text{Ni}(\text{CN})_4$. *Inorg. Chim. Acta* **2015**, *426*, 142–145.
52. Koenig, E.; Madeja, K. $5T_2-1A_1$ Equilibriums in some iron(II)-bis(1,10-phenanthroline) complexes. *Inorg. Chem.* **1967**, *6*, 48–55, doi:10.1021/ic50047a011.
53. Gütlich, Philipp, G.H.A. *Spin Crossover in Transition Metal Compounds I*; Springer: Berlin, Germany, 2004.
54. Molnár, G.; Kitazawa, T.; Dubrovinsky, L.; McGarvey, J.J.; Bousseksou, A. Pressure tuning Raman spectroscopy of the spin crossover coordination polymer $\text{Fe}(\text{C}_5\text{H}_5\text{N})_2[\text{Ni}(\text{CN})_4]$. *J. Phys. Condens. Matter* **2004**, *16*, S1129.
55. Tuchagues, J.P.; Bousseksou, A.; Molnár, G.; McGarvey, J.J.; Varret, F. The Role of Molecular Vibrations in the Spin Crossover Phenomenon. In *Spin Crossover in Transition Metal Compounds III*; Springer: Berlin/Heidelberg, Germany, 2004; pp. 84–103.
56. Hauser, A. Light-Induced Spin Crossover and the High-Spin→Low-Spin Relaxation. In *Spin Crossover in Transition Metal Compounds II*; Springer: Berlin/Heidelberg, Germany, 2004; pp. 155–198.
57. Krivokapic, I.; Zerara, M.; Daku, M.L.; Vargas, A.; Enachescu, C.; Ambrus, C.; Tregenna-Piggott, P.; Amstutz, N.; Krausz, E.; Hauser, A. Spin-crossover in cobalt(II) imine complexes. *Coord. Chem. Rev.* **2007**, *251*, 364–378.
58. Gütlich, P.; Gaspar, A.B.; Garcia, Y. Spin state switching in iron coordination compounds. *Beilstein J. Org. Chem.* **2013**, *9*, 342–391.
59. Decurtins, S.; Gütlich, P.; Köhler, C.; Spiering, H.; Hauser, A. Light-induced excited spin state trapping in a transition-metal complex: The hexa-1-propyltetrazole-iron(II) tetrafluoroborate spin-crossover system. *Chem. Phys. Lett.* **1984**, *105*, 1–4.
60. Hauser, A. Reversibility of light-induced excited spin state trapping in the $\text{Fe}(\text{ptz})_6(\text{BF}_4)_2$, and the $\text{Zn}_{1-x}\text{Fe}_x(\text{ptz})_6(\text{BF}_4)_2$ spin-crossover systems. *Chem. Phys. Lett.* **1986**, *124*, 543–548.
61. Létard, J.F.; Capes, L.; Chastanet, G.; Moliner, N.; Létard, S.; Real, J.A.; Kahn, O. Critical temperature of the LIESST effect in iron(II) spin crossover compounds. *Chem. Phys. Lett.* **1999**, *313*, 115–120.
62. Enachescu, C.; Machado, H.; Menendez, N.; Codjovi, E.; Linares, J.; Varret, F.; Stancu, A. Static and light induced hysteresis in spin-crossover compounds: Experimental data and application of Preisach-type models. *Phys. B Condens. Matter* **2001**, *306*, 155–160.
63. Baldé, C.; Bauer, W.; Kaps, E.; Neville, S.; Desplanches, C.; Chastanet, G.; Weber, B.; Létard, J.F. Light-Induced Excited Spin-State Properties in 1D Iron(II) Chain Compounds. *Eur. J. Inorg. Chem.* **2013**, *2013*, 2744–2750.
64. Weber, B.; Tandon, R.; Himsl, D. Synthesis, Magnetic Properties and X-ray Structure Analysis of a 1-D Chain Iron(II) Spin Crossover Complex with wide Hysteresis. *Zeitschrift für Anorganische und Allgemeine Chemie* **2007**, *633*, 1159–1162.
65. Bauer, W.; Scherer, W.; Altmannshofer, S.; Weber, B. Two-Step versus One-Step Spin Transitions in Iron(II) 1D Chain Compounds. *Eur. J. Inorg. Chem.* **2011**, *2011*, 2803–2818.
66. Weber, B.; Kaps, E.S.; Desplanches, C.; Létard, J.F. Quenching the Hysteresis in Single Crystals of a 1D Chain Iron(II) Spin Crossover Complex. *Eur. J. Inorg. Chem.* **2008**, *2008*, 2963–2966.
67. Boukheddaden, K.; Miyashita, S.; Nishino, M. Elastic interaction among transition metals in one-dimensional spin-crossover solids. *Phys. Rev. B* **2007**, *75*, 094112.
68. Willenbacher, N.; Spiering, H. The elastic interaction of high-spin and low-spin complex molecules in spin-crossover compounds. *J. Phys. C Solid State Phys.* **1988**, *21*, 1423–1439.
69. Spiering, H.; Willenbacher, N. Elastic interaction of high-spin and low-spin complex molecules in spin-crossover compounds. II. *J. Phys. Condens. Matter* **1989**, *1*, 10089–10105.
70. Spiering, H.; Boukheddaden, K.; Linares, J.; Varret, F. Total free energy of a spin-crossover molecular system. *Phys. Rev. B* **2004**, *70*, 184106.
71. Banerjee, H.; Kumar, M.; Saha-Dasgupta, T. Cooperativity in spin-crossover transition in metalorganic complexes: Interplay of magnetic and elastic interactions. *Phys. Rev. B* **2014**, *90*, 174433.
72. Timm, C. Collective effects in spin-crossover chains with exchange interaction. *Phys. Rev. B* **2006**, *73*, 014423.
73. D'Avino, G.; Painelli, A.; Boukheddaden, K. Vibronic model for spin crossover complexes. *Phys. Rev. B* **2011**, *84*, 104119.
74. Miralles, J.; Castell, O.; Caballol, R.; Malrieu, J.P. Specific CI calculation of energy differences: Transition energies and bond energies. *Chem. Phys.* **1993**, *172*, 33–43.
75. Roos, B.O.; Taylor, P.R.; Siegbahn, P.E. A complete active space SCF method (CASSCF) using a density matrix formulated super-CI approach. *Chem. Phys.* **1980**, *48*, 157–173.

76. Fouqueau, A.; Mer, S.; Casida, M.E.; Daku, L.M.L.; Hauser, A.; Mineva, T.; Neese, F. Comparison of density functionals for energy and structural differences between the high- $[5T_{2g}:(t_{2g})^4(e_g)^2]$ and low- $[1A_{1g}:(t_{2g})^6(e_g)^0]$ spin states of the hexaquoferrous cation $[\text{Fe}(\text{H}_2\text{O})_6]^{2+}$. *J. Chem. Phys.* **2004**, *120*, 9473–9486, doi:10.1063/1.1710046.
77. Ordejón, B.; de Graaf, C.; Sousa, C. Light-Induced Excited-State Spin Trapping in Tetrazole-Based Spin Crossover Systems. *J. Am. Chem. Soc.* **2008**, *130*, 13961–13968, doi:10.1021/ja804506h.
78. Pierloot, K.; Vancoillie, S. Relative energy of the high- (T_{2g}^5) and low- (A_{1g}^1) spin states of $[\text{Fe}(\text{H}_2\text{O})_6]^{2+}$, $[\text{Fe}(\text{NH}_3)_6]^{2+}$, and $[\text{Fe}(\text{bpy})_3]^{2+}$: CASPT2 versus density functional theory. *J. Chem. Phys.* **2006**, *125*, 124303, doi:10.1063/1.2353829.
79. Watts, J.D.; Gauss, J.; Bartlett, R.J. Coupled cluster methods with noniterative triple excitations for restricted open shell Hartree Fock and other general single determinant reference functions. Energies and analytical gradients. *J. Chem. Phys.* **1993**, *98*, 8718–8733, doi:10.1063/1.464480.
80. Maldonado, P.; Kanungo, S.; Saha-Dasgupta, T.; Oppeneer, P.M. Two-step spin-switchable tetranuclear Fe(II) molecular solid: Ab initio theory and predictions. *Phys. Rev. B* **2013**, *88*, 020408.
81. Sarkar, S.; Tarafder, K.; Oppeneer, P.M.; Saha-Dasgupta, T. Spin-crossover in cyanide-based bimetallic coordination polymers—insight from first-principles calculations. *J. Mater. Chem.* **2011**, *21*, 13832–13840.
82. Jeschke, H.O.; Salguero, L.A.; Rahaman, B.; Buchsbaum, C.; Pashchenko, V.; Schmidt, M.U.; Saha-Dasgupta, T.; Valentí, R. Microscopic modeling of a spin crossover transition. *New J. Phys.* **2007**, *9*, 448.
83. Tarafder, K.; Kanungo, S.; Oppeneer, P.M.; Saha-Dasgupta, T. Pressure and Temperature Control of Spin-Switchable Metal–Organic Coordination Polymers from Ab Initio Calculations. *Phys. Rev. Lett.* **2012**, *109*, 077203.
84. Dudarev, S.L.; Botton, G.A.; Savrasov, S.Y.; Humphreys, C.J.; Sutton, A.P. Electron-energy-loss spectra and the structural stability of nickel oxide: An LSDA+U study. *Phys. Rev. B* **1998**, *57*, 1505–1509.
85. Alvarez, S. Distortion Pathways of Transition Metal Coordination Polyhedra Induced by Chelating Topology. *Chem. Rev.* **2015**, *115*, 13447–13483, doi:10.1021/acs.chemrev.5b00537.
86. Kresse, G.; Hafner, J. Ab initio molecular-dynamics simulation of the liquid-metal-amorphous-semiconductor transition in germanium. *Phys. Rev. B* **1994**, *49*, 14251–14269.
87. Kresse, G.; Furthmüller, J. Efficient iterative schemes for ab initio total-energy calculations using a plane-wave basis set. *Phys. Rev. B* **1996**, *54*, 11169–11186.
88. Perdew, J.P.; Burke, K.; Ernzerhof, M. Generalized Gradient Approximation Made Simple. *Phys. Rev. Lett.* **1996**, *77*, 3865–3868.
89. Buhks, E.; Navon, G.; Bixon, M.; Jortner, J. Spin conversion processes in solutions. *J. Am. Chem. Soc.* **1980**, *102*, 2918–2923, doi:10.1021/ja00529a009.
90. Hauser, A.; Guetlich, P.; Spiering, H. High-spin fwdarw low-spin relaxation kinetics and cooperative effects in the hexakis(1-propyltetrazole)iron bis(tetrafluoroborate) and $[\text{Zn}_{1-x}\text{Fe}_x(\text{ptz})_6](\text{BF}_4)_2$ (ptz = 1-propyltetrazole) spin-crossover systems. *Inorg. Chem.* **1986**, *25*, 4245–4248, doi:10.1021/ic00243a036.
91. Létard, J.F.; Guionneau, P.; Rabardel, L.; Howard, J.A.K.; Goeta, A.E.; Chasseau, D.; Kahn, O. Structural, Magnetic, and Photomagnetic Studies of a Mononuclear Iron(II) Derivative Exhibiting an Exceptionally Abrupt Spin Transition. Light-Induced Thermal Hysteresis Phenomenon. *Inorg. Chem.* **1998**, *37*, 4432–4441, doi:10.1021/ic980107b, PMID:11670580.
92. Morgan, G.G.; Murnaghan, K.D.; Müller-Bunz, H.; McKee, V.; Harding, C.J. A Manganese(III) Complex that Exhibits Spin Crossover Triggered by Geometric Tuning. *Angew. Chem.* **2006**, *118*, 7350–7353.
93. Martinho, P.N.; Gildea, B.; Harris, M.M.; Lemma, T.; Naik, A.D.; Müller-Bunz, H.; Keyes, T.E.; Garcia, Y.; Morgan, G.G. Cooperative Spin Transition in a Mononuclear Manganese(III) Complex. *Angew. Chem.* **2012**, *124*, 12765–12769.

